Developments and Applications of a New Type Test Chart for Radiographic Image Quality Measurement.

Yuhsaku Tamoto and Eitaro Kubo
Research & Development Laboratory, Konishiroku Photo Ind. Co., Ltd.

放射線画像測定用新型テストチャートの試作と応用

小西六写真工業株式会社　開発研究所
田本祐作　久保栄太郎

（昭和45年4月7日受付）

放射線画像の鮮鋭度を測定するためにアルミニウム箔と鉛箔とでパターンを構成する全金属製の矩形波チャート（パターンの厚さ1㎜，最高周波数10 lines/mm）を試作し，これのコントラストおよび入射角度特性について検討を加えた．その結果，このチャートは従来の蒸着型チャートがコントラスト C_E ≒0.5であるのに比べて C_E =0.9以上の高いコントラストを持つことが判明した．

また，入射角度特性を検討した結果，チャートの厚さによつて斜入射X線をさえぎる割合を示す係数ηの値が蒸着型チャートの約20倍という大きな値を示す割にはレスポンス関数の低下が少なく，この角度特性の点でも優れた特性を示していることが確かめられた．

さらに，われわれは人体中の疾患部をこの試作チャートでSimulateし，それとX線フィルムとの距離（cfd）によつて，その画像の鮮鋭度が変化する状況をレスポンス関数の測定を用いて検討した．その結果cfdと鮮鋭度との相対的な関係をレスポンス関数によつて定量的に求めることができた．

Summary

A rectangular-waveformed test chart (thickness of pattern: 1.0 mm, and maximum frequency: 10 lines/mm) constituted of patterns of aluminum and lead foils for measuring the sharpness of radiographic images was trially made and the contrast and the incident angle characteristics were examined. As a result it was clarified that the contrast of chart C_E is larger than 0.9 compared with the value 0.5 of the conventional evaporation-type test chart. As for the incident angle characteristics, the excellence of our trially made test chart was confirmed from the fact that though the coefficient η indicating the rate of interruption of oblique incident X-ray gave a value as large as about 20 times the value of the evaporation-type test chart and the lowering of the response function remained small.

Furthermore, we simulated a diseased part of the human body with this trially-made test chart (we call this KR-chart) and we examined the changes of the response functions which characterized the diseased part image quality corresponding to the changes of the distances between the test chart which simulated the diseased part and the X-ray film, we express ed this distance cfd for brevity. In this way we were able to obtain a relation between the cfd and the sharpness quantitatively in terms of the response function.

1. Introduction

It is well-known that, in the evaluation of sharpness of a photographic image, the use of response function is an effective method in general. There are several experimental procedures to obtain such a response function, and they can be divided into two ways, one is a method to apply Fourier transformation to the intensity distribution of an edge image or a slit image, and the other is a method to employ a test chart, that is, a pattern in which the contrast is definite and the frequency varies spatially. The method of applying Fourier transformation is being carried out fairly much in laboratories, and the method of employing test chart has advantages such that, compared with the former, the measuring method is simple, the accuracy is stable, and the resolving power can be read out immediately under a microscope. Generally speaking, the data of response function are usually inaccurate near the cut-off frequency to make it difficult to presume the marginal resolving power from the curve of response function. On the other hand in the test chart method, both of them can be obtained simultaneously, so that, from this point of view, this method is used widely in the optical field as an expedient more than usual Fourier transformation method. In the measurement of sharpness of radiographic image, mainly in the measurement of X-ray photographic image, the effectiveness of the test chart measuring system is now recognizing. But in spite of the fact that the test chart plays a very important role in the image sharpness measurement, its manufucturing process are not so easy as in a test chart generally used in the optical field, because of the speciality of radiation photography. In the case of usual photography, the material of these chart sufficiently fulfills the qualification required as a test chart by use of a photographic film and the like, but in the case of radiation photography, it becomes necessary to combine a material of hardly transmitting radiation such as, lead and platinum with a material of transmitting radiation comparatively well such as synthetic resin or glass.

This means that the manufacturing process of chart are exceedingly difficult compared with the materials used in the usual photography. According to the conventional manufacturing process, the pattern part is usually made of metal and the supporter of pattern is made of radiation transmitting material, and from the point of working accuracy, the edges of pattern will become less accurate as the frequency is increased, so that the thickness of metallic pattern is limited at about 50 μ in maximum in a chart of maximum frequency of about 10 lines/mm. However, this thickness is not enough to use for a chart of high contrast suitable for the measurement of sharpness because of less absorption of radiation. As far as we are aware of, a chart giving an sufficiently high contrast seems not to be available at present.

This report relates to a series of our investigation for solving problems mentioned above, namely, a unique manufacturing process of high contrast chart (to be abbreviated as KR-chart hereafter) used for measuring the sharpness of radiographic image and its application.

2. Manufacturing

Our trially made KR-chart is an all-over metallic chart consisting of rectangular wave patterns, in which lead foils were used as radiation absorbing material and aluminum foils as radiation penetrating material. The KR-chart is shown in Fig.1. Its manufacturing process can be divided into 7 steps as shown in a flow-chart of Fig. 2. In the following the process will be explained according to the flow-chart.

1. Material selection step

At first, in order to obtain a pattern of required spatial frequency ν_n, metallic foils with thickness

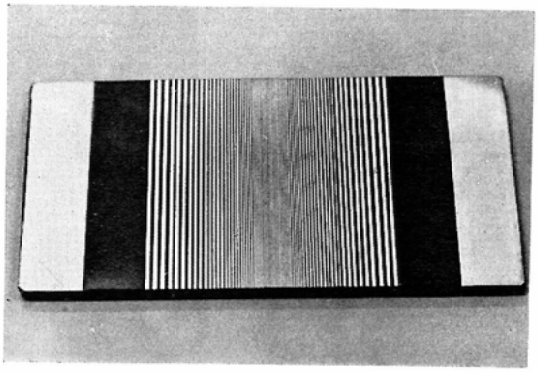

Fig. 1. The photograph of a new type test chart developed for radiographic image quality measurement.

corresponding to the frequency are selected with a micrometer.

2. Material cleaning step

Remove the contamination of oil and others attached to the metallic foils. In the subsequent steps, this removal is necessary for the purpose of making better the adhesion between the foils themselves. The aluminum foils are treated with a supersonic washing machine in which trichlene liquid is used, and the lead foils are treated with a vapor shower washing machine in which the same liquid is used, too. In this way the surfaces of materials are cleaned well.

3. Adhesive coating step

After the metallic foils are made to pass between special rollers coated with a thermo-hardening epoxy adhesive resin, the adhesive is easily dried by applying the heating of 130°C for 20 min.

This is a kind of pre-treatment for the next step of cutting the metallic foils into fine pieces, bcause the coating of adhesive would be difficult if it would be done after the next step.

4. Cutting step

In this step the thickness of pattern part of KR-chart is nearly determined. In cutting, a special cutting machine devised not to distort fine metallic foils is used for shearing.

In thi sstep the cutting of foils was done at width of 3.0 mm.

5. Setting and adhering step

Using a special setting machine the pattern part of KR-chart is set up by keeping the cut metallic fine pieces in parallel each other and perpendicular to the base plate, and the aluminum and lead foils are alternately arranged according to the order of arrangement of specified spatial frequency. Then they are heated in an electric oven at 250°C for 60—90 min and made to adhere, thereby the underdried adhesive is perfectly thermo-hardened and a prototype of pattern part is finished.

6. Plainly shaping step

In the steps described above the pattern of 3.0 mm thickness has been set up and the thickness of pattern part of KR-chart is completed exactly in this step. Actually the plane shaping is performed with a shaper, and the minimum marginal thickness of this finished pattern is 1.0 mm in the present practice.

7. Finish-working step

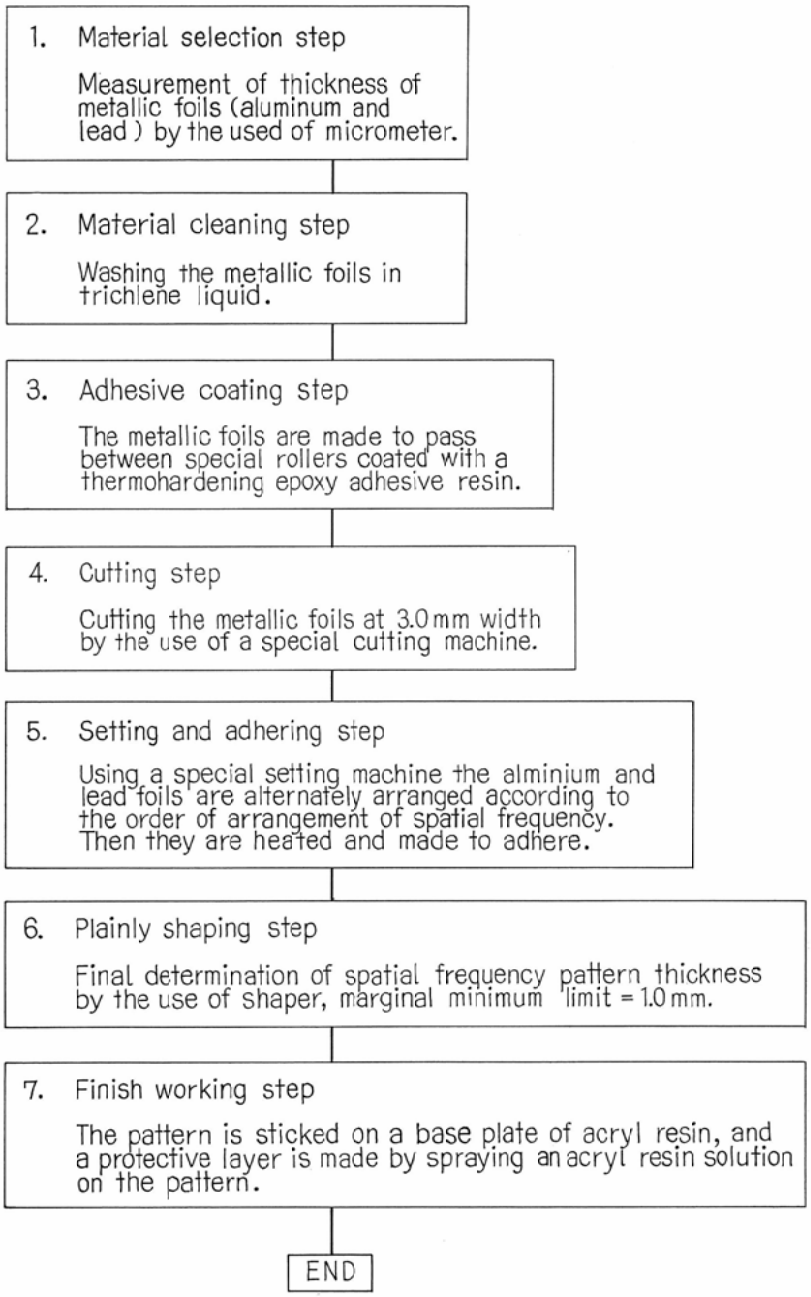

Fig. 2. The KR-chart manufacturing process can be divided into 7 stps as shown in this flow-chart.

In this final step the pattern is sticked on a base plate of acryl resin 1.0 mm thick, and, by spraying a transparent acryl resin solution on the pattern to make a protective layer, the KR-chart is manufactured completely.

In the above the flow of manufacturing process has been outlined, in which the steps 4—6 are the main parts showing the special features of the KR-chart manufacturing process, so that a supplemental explanation is given referring to Fig. 3. In the step 4 shown in the figure the aluminum and lead foils are divided into blocks Bn (n=1,2,…)of the same thickness D-mm, at first, then each one piece belonging to this block is cut into pieces of Zmm width. In this case Z was taken equal to 3.0 mm. In the step 5 the aluminum and lead foils are overlapped alternately in each block using the setting machine and further by combining these blocks, a rectangular wave pattern as shown in the figure is formed. After heating and adhering treatments being applied, the pattern is transferred to the step 6. What determines the spatial frequency ν_n lines/mm is the thicknesses of metallic foils Dn mm and there is a relation $\nu_n = 1/2 \cdot D_n$ between them. The number of repetition of same frequency is determined by the number of pairs in the block (cf. Table 1).

Type	Spatial Frequency (Lines/mm) Pair (n)	X (mm)	Y (mm)	Z_1 (mm)	Z_2 (mm)
RF-type KR-chart	0.0 (1), 0.05 (1), 0.85 (3), 1.0 (3), 1.25 (3), 1.65 (3), 2.0 (3), 2.5 (5), 3.0 (5), 5.0 (5), and 10.0 (5)	80	40	1.0	1.0
RP-type KR-chart	0.0 (1), 0.025 (1), 0.75 (8), 1.5 (30), 2.0 (40), 2.5 (50), 3.0 (60), 5.0 (100), and 10.0 (100)	220	60	1.0	1.0

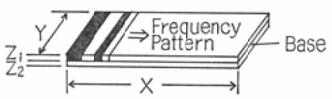

Table 1. Shown the dimension and arrangement of the KR-chart.

The order of arrangement of patterns for each frequency can be changed by the manner of arrangement of blocks, for example, the two kinds of X-ray photography of patterns desired by the designer as shown in Fig. 4 can be obtained.

The photograph (A) represents a KR-chart (RP-type KR-chart) used for the measurement of radiographic image resolving power, in which the mark lines of 3.0 mm wide (of aluminum pieces) are inserted to discriminate the patterns of different spatial frequency (rectangular frequency). The photograph (B) corresponds to another KR-chart (RF-type KR-chart) used mainly for the measurement of response function, in which the number of repetition of the same frequency is less compared with (A) and the arrangement is symmetry on both sides. In Table 1 there are shown the frequency arrangement of the RP-and RF-types of KR-charts and the dimensions of each element of these charts.

In the step 6 the plainly shaping process is applied to obtain a pattern with smaller thickness than the minimum marginal thickness of cutting width, i.e., 3.0 mm; namely the part shown by the dashed lines of

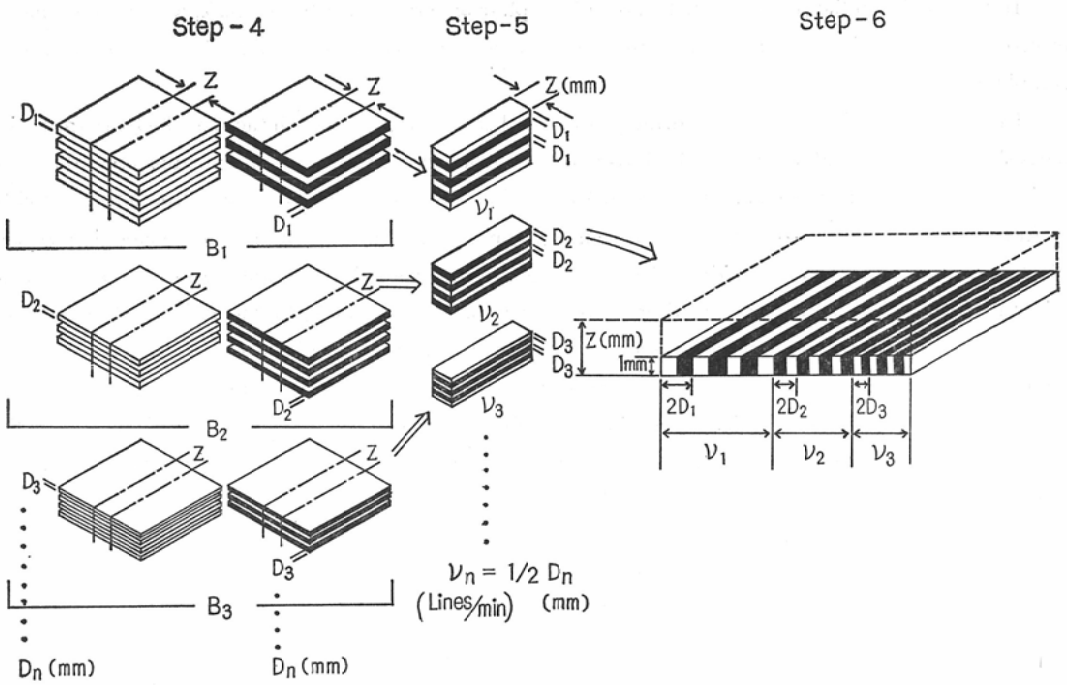

Fig. 3. The schematic diagram of the main parts in the flow-chart (Fig. 2) of the KR-chart manufacturing process.

Fig. 3 is removed, thereby a pattern part of KR-chart having a finished thickness of 1.0 mm is accomplished.

3. Performance

3–1. Chart contrast

As an experimental method of observing the contrast of the charts produced in the above procedure, the X-ray photographic method was employed. In this case a typical evaporation-type test chart (to be abbreviated as SR-chart hereafter) was selected as a reference from among some kinds of commercial radiologic charts for the following comparison tests. Generally the evaporation-type test charts are made in such a way that a lead layer is deposited on a base plate made of synthetic resin and the arrangement of its spatial frequency pattern is made by the photographic etching process or mechanical working process. The lead layer has usually a thickness of the order of 50 μ.

3–1–1. Experimental procedure

KR-chart and SR-chart were put side by side on an X-ray film and photographed simultaneously and then were measured the photographic density of each image at the zero frequency, and the chart contrast C_E was calculated by the following formula;

$$C_E = \frac{E_{max} - E_{min}}{E_{max} + E_{min}} \qquad (1)$$

where E_{max} and E_{min} denote respectively the reduced maximum and minimum X-ray intensities converted from the maximum and minimum photographic densities D_{max} and D_{min} at the X-ray penetrating and absorbing parts both correspond to $\nu = 0$ line/mm using the photographic characteristic curve. These

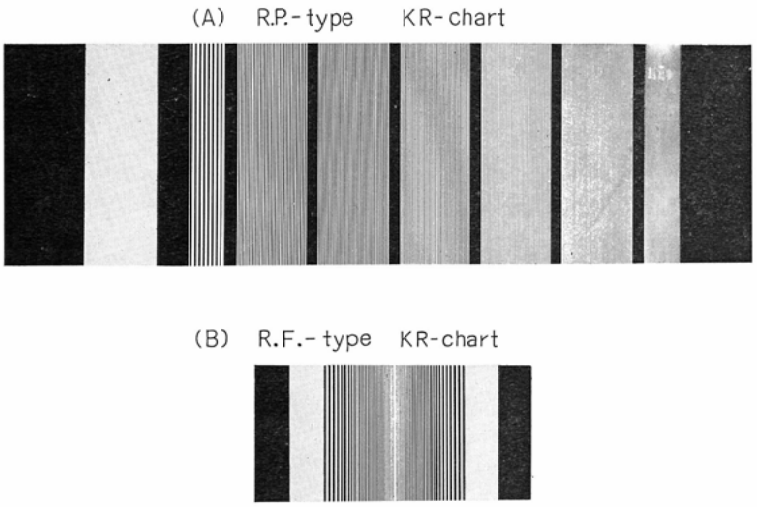

Fig. 4. The X-ray photograph (A) represents a RP-type KR-chart used for the measurement of radiographic image resolving power, and (B) represents a RF-type KR-chart used mainly for the measurement of response function.

E_{max} and E_{min} never take negative values, so that, the maximum value of C_E is 1.0. Therefore, if E_{max} is definite C_E tends to zero when E_{min} approaches a larger value. The range of chart contrast to be examined is limited in the photographic density range used for usual diagnosis in this case D_{max} ranges from 0.5 to 2.0 and the X-ray tube voltage ranges from 50 to 100 kVp. The films used were Sakura X-ray films of New Y-type for medical use, and the X-ray source used was an X-ray generating device made in Toshiba Electric Co., Ltd., KXO-15-2A type for medical use.

In taking a photograph the distance between the X-ray source and the film was fixed at 200 cm and each KR and SR-chart was placed in contact with the X-ray film to undergo the comparison test. Under a constant voltage of X-ray tube the photographs were taken one at a time for different exposure values, by changing the X-ray tube current, exchanging the films successively and taking the exposure value as a parameter. Next, a similar photographing was done by changing the X-ray tube voltage. Thus the data of a series of measurements for various X-ray tube voltages and X-ray doses were obtained. The development was performed by the use of Sakura high speed automatic developer QX-200 and the density of image was measured by means of Sakura photoelectric densitometer of PD-5 type.

3–1–2. Results of measurement and considerations

The results of measurement of photographic density are shown in Fig. 5—7. In Fig. 5 and 6 there are given the measured values of photographic density covering the whole range of examination of chart contrast, in other words characteristic surfaces of photographic density against tube voltage and exposure value corresponding to KR and SR-chart are given respectively in these figures. From the D_{min} surfaces represented by dashed lines the difference in both charts is clearly observed. Namely, in the case of KR-chart, D_{min} is extremely low throughout the whole range showing the values nearly equal to the values of density of films (film base density + fog density), whereas in the case of SR-chart the rate of increase of D_{min} values in associated with the increase of X-ray tube voltages and exposure values

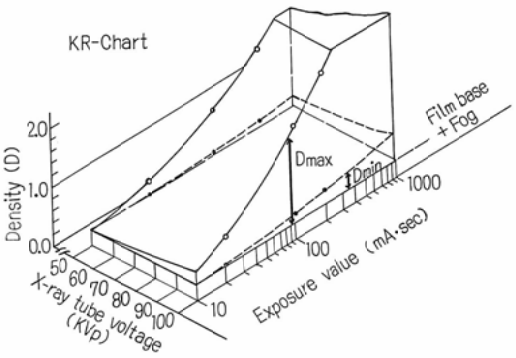

Fig. 5. The results of measurement of photographic density covering the whole range of examination of chart contrast of the KR-chart.

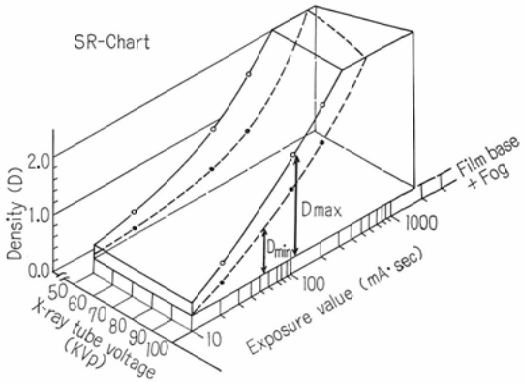

Fig. 6. The results of measurement of photographic density covering the whole range of examination of chart contrast of the SR-chart.

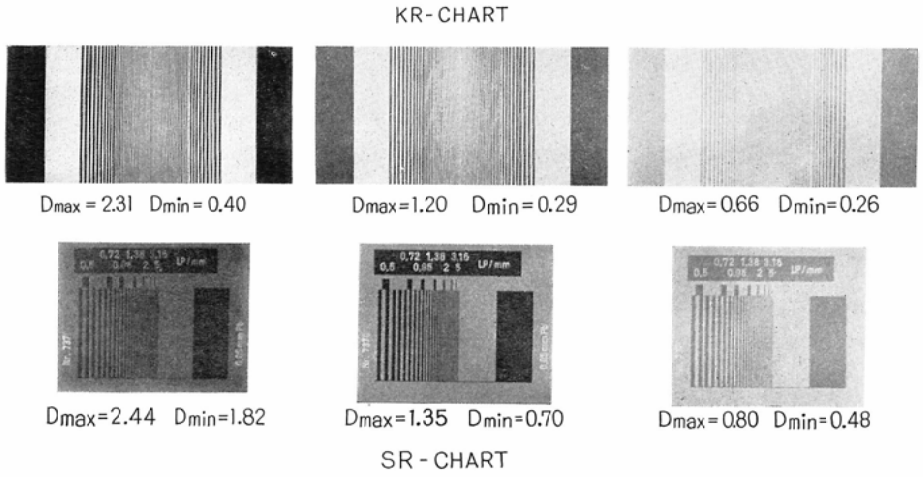

Fig. 7. The photographic sample for the chart contrast measurement used for obtaining the graphs in Fig. 5, 6.

is very remarkable. These circumstances are evidently understood from the photographs of Fig. 7, too.

To support these considerations quantitatively, the results of calculation of chart contrast C_E obtained by the formula (1) are shown in Fig. 8. According to the results the value of C_E for the SR-chart is less than 0.7, so that it seems better to use this chart as a half-contrast or low-contrast chart rather than as a high-contrast chart.

On the other hand, in the KR-chart the value of C_E is lager than 0.9 over the whole ranges of measuring factors (X-ray tube voltage, resultant photographic density) as evidently seen from Fig. 8, therefore it is confirmed that the KR-chart can be used for measuring the sharpness of high contrast X-ray image in usual diagnosis with sufficiently high contrast.

3–2. Incident angle characteristics

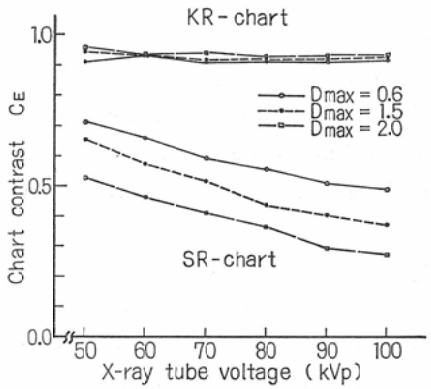

Fig. 8. The result of chart contrast C_E vs X-ray tube voltage characteristic curves from the data shown in Fig. 5, 6.

The KR-chart is composed of a series of spatial frequency patterns with 1.0 mm thickness to satisfy its high contrast character. In this case the ratio of the line breadth and the thickness of the pattern at maximum frequency $\nu_{max} = 10$ lines/mm becomes 1/20.

When this ratio is large, the aspect of radiation incident upon the test chart is considered to resemble a circumstance of the sunlight incident upon a valley of buildings. Therefore, depending on the incident angle of light a part corresponding to the shade appears and sometimes makes it impossible to transmit precisely the spatial frequency wave pattern suitable for a test chart to the measured system (X-ray film emulsion). To examine such influence the incident angle characteristics, i.e., the state of variation of the sqaure wave response function(to be abbreviated as SWR hereafter)of X-ray film is investigated in the fol-

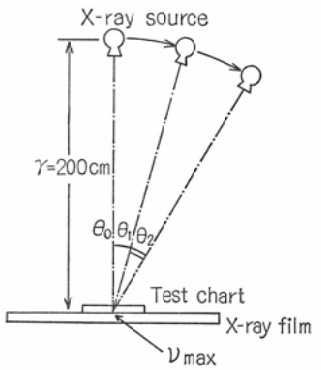

Fig. 9(A) The geometrical exposure arrangement of the incident X-ray angle variation.

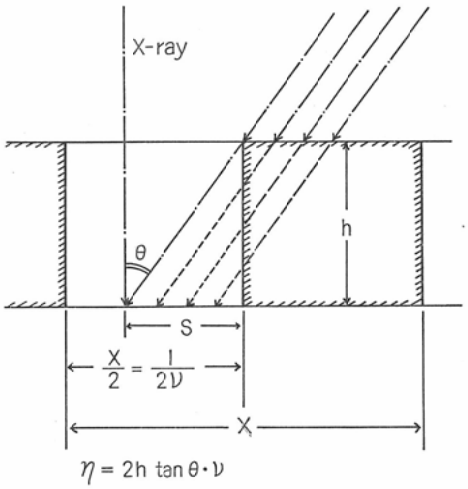

Fig. 9(B) The aspect of the X-ray incidence to the X-ray film emulsion through the chart, and the coefficient η which indicates the interruption ratio of the oblique incidence X-ray can be calculated with the formula which involves such parameters θ, ν, h, in this figure.

lowing.

3–2–1. Experimental method

The experiments were performed under the conditions shown in Fig. 9(A). To simplify the problem, the distance between the film and the X-ray source was fixed at 200 cm and it was far larger than the dimension of chart. Therefore it is sufficient to consider only the influence of incident angle with chart due to the main part of X-ray coming along the main axis of exposing radiation cone, and this aspect may be seen in Fig. 9(B).

As the influence of incident angle is generally predominant in the part of higher frequency of this chart so in our experiments the exposure was done in such a way that the intersection between the main axis of exposing radiation cone of incident X-ray and the chart surface was fixed always at the position of maximum frequency of 10 lines/mm and the X-ray source was moved along the periphery of a circle of r=200 cm as shown in Fig. 9(A). The photographing condition other than this geometrical one was kept entirely the same throughout our experiments. Let us denote the ratio of the shady part S in Fig. 9(B) to the width of X-ray transmitting metallic foil X/2 by a coefficient η.

In the present case, if the X-ray in the part S is assumed to be perfectly shaded by neglecting entirely the differences of radiation intensities in the part S due to the differences of radiation pathes in the X-ray absorbing metallic foil shown by the dashed lines, the coefficient η can be expressed by using the incident angle θ, the spatial frequency of chart ν, and the thickness of chart h as follows;

$$\eta = 2h \tan \theta \cdot \nu \qquad (2)$$

when $\eta = 0$ it means vertical incidence and the case of $\eta = 1.0$ corresponds to perfect interruption of X rays.

Here the procedure of measurement of SWR followed the method to be described in section 4.1, and the experiment for SR-chart was made by the same procedure.

3–2–2. Results of measurement and consideration

The results of measurement on the variation of SWR along the change of incident angle is shown in Fig. 10. The measurements were done at 3 points, i.e., $\theta = 0°$, $\theta = 2.9°$, and $\theta = 5.7°$. The full lines represent the SWR of KR-chart and the dashed lines the SWR of SR-chart. The values of η are dif-

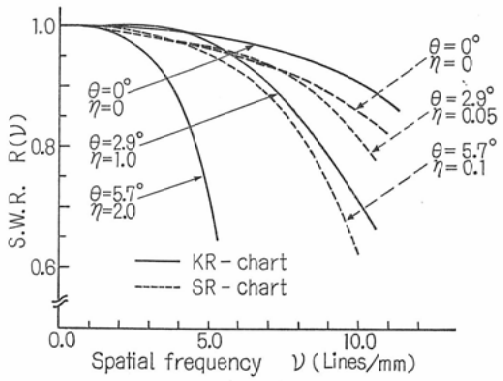

Fig. 10. The results of measurement on the variation of SWR (square wave response) along the change of incident angle.

ferent at the same angle according to the charts, for example, in the case of $\theta = 2.9°$ the values of η are 1.0 and 0.05 for in the KR-chart and the SR-chart respectively. It is to be noticed however that, since in the case of $\theta = 2.9°$ the value of η is 1.0 for the KR-chart, the X-ray is perfectly interrupted in the KR-chart as mentioned above, so that the calculated value of SWR must be equal to zero, whereas the experimental value of SWR for this KR-chart is given by about 0.7 as seen in the figure, and this damping shows only about 20% attenuation compared with the value of SWR at the same 10 lines/mm in the normal incidence i.e., at $\theta = 0°$.

This means that in the case of KR-chart the incident angle characteristic would not be significant so much.

On the other hand, since in the case of SR-chart the pattern is composed of a thin lead layer evaporated about 50 μ, the variation of η due to the change of incident angle should be very small compared with the KR-chart.

For example, the value of η amounts to 0.05 for $\theta = 2.9°$ and only 0.1 even for $\theta = 5.7°$. It can therefore be inferred that the values of SWR along the variation of incident angle of X-ray measured by the use of such an evaporation-type chart as mentioned above would give a better chracteristics rather than our KR-chart.

However, according to the experimental results obtained, this inference is not always true, namely, in spite of the value of η at $\theta = 5.7°$ being only 0.1 in the SR-chart, the value of SWR is given by about 0.65 at the frequency of 10 lines/mm, in other words, there is brought about lowering of SWR value of the same order as in the case of KR-chart where the value of SWR corresponding to the value of $\eta = 1.0$ has been 0.7, thereby it is recognized that, in the case of SR-chart, the incident angle characteristic gives a remarkably large effect as compared with the case of KR-chart.

This difference may probably comes from the difference of manufacturing process of chart pattern, that is, in the case of SR-chart the metallic lead deposited on the support has a porous structure differently from the foils of lead, so that the X-ray absorption of the former is considered not to affect so effectively as in the latter.

The above mentioned experimental facts are summarized as follows:

Supposing that the inclination of incident angle of X-ray is the same, the KR-chart with pattern 1.0 mm thick and the SR-chart with pattern about 50 μ thick have different percentages of the shady part shown in Fig. 9(b) respectively, and they are indicated by the different values of η.

In the case of same incident angle and the same position of frequency patterns the value of η of SR-chart relative to the value of η of KR-chart is always obtained 0.05 by the use of formula (2) because of the chart thickness (h).

Generally it is expected that the larger value of η brings about the larger value of attenuation of SWR, but as metallic foils are used in the KR-chart, this attenuation of SWR value is rather small for the larger value of η, and hence the fact that the KR-chart has an excellent incident angle characteristic compared with the evaporation-type chart has been confirmed.

4. Applied measurement

In the detection of a deseased part by the use of X-ray photography for diagnosis, it is necessary to grasp, a change of shape, for example, the fracture of bone on the image, or the visual difference of

Xray absorbing situation of normal and abnormal tissue in human body is displayed on the image as a difference of photographic density.

Therefore, the sharpness of image affects the accuracy of diagnosis by the use of the X-ray photograph. In a sharp X-ray photograph, it is possible to detect even a very fine diseased part, but in an obscure X-ray photograph it is very difficult to defect such a fine diseased part because of the less accuracy of the image.

In treating the unsharpness of image quantitatively, the response function affords a powerful method[1)2)].

In order to investigate quantitatively the degree of unsharpness of image produced by changing "the distance between the photographed body and film" we measured the SWR which is the response function for rectangular wave by the use of KR-chart.

In the case of existence of diseased parts in a human body, we made experiments to how the spatial frequency spectrum for X-ray photograph is changed along the position of diseased part namely by changing the distance between the photographed body and the film, and by using a KR-chart as a simulator of the diseased parts for certain distances between the photographed body and the film.

Where, we have been supposed, for example, abnormal parts of bone tissues as the simulated diseased parts.

4–1. Experimental method

The experiment was carried out as shown in Fig. 11. In place of the living body a chest phantom

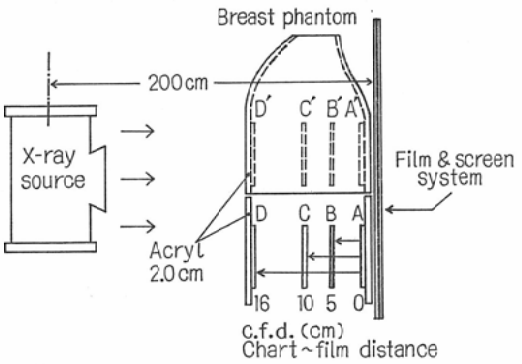

Fig. 11. The schematic diagram of application measurement used KR-chart.

made of synthetic resin is used. Supposing in the interior of the phantom the diseased part indicated by the dashed lines A′ B′ C′ D′ in the figure respectively and taking X-ray photographs one by one under the same exposure condition in each time when the KR-chart is placed at each position of the phantom, it is expected that fairly resembling results would be obtained as in the case of diseased part photographing on the actual living body. It is also expected however that, since in the photographs thus obtained the image of bone structure of breast part is naturally superposed on that of the KR-chart, if we intend to derive the response function corresponding to each diseased part by the use of photographs, the bone part would become a disturbing shade, causing a difficulty in the scanning operation using a micro-densitometer.

To resolve this difficulty, we mounted a holder made of acryl resin under the chest phantom as shown in Fig. 11, determining this holder thickness so as to have absorbing amount for X-ray approximately equal

to that of the chest phantom, and took photographs for measuring the response function in such improved situation where the bone structure was eliminated.

The experimental conditions in this case were as follows: X-ray sourse: Toshiba KXO-15-2A type with focal size 1×1 mm, film: Sakura X-ray film New Y-Type, fluorescent screen: Kyokko FS, synthetic resin phantom made of 3M Co., Ltd. was used as chest phantom.

The photographing conditions were: Distance between X-ray source and film = 200 cm, X-ray tube voltage = 150 kVp, X-ray tube current = 200 mA, exposure time = 0.08 sec. Development was done with Sakura QX-200 high speed automatic developing unit and the measuring device was Sakura micro-densitometer PDM—2401 type used under the condition of scanning slit of $10\,\mu \times 200\,\mu$.

The procedure of measuring the response function was as following: At first the photographic density waveform D (ν) of each sample was obtained on a recording paper by tracing with the micro-densitometer.

On the other hand, a sample that had been photographed an aluminum wedge independently of above mentioned procedure was traced with the micro-densitometer to get a photographic characteristic curve, and by the use of this curve the density waveform D (ν) mentioned above was transformed into a reduced X-ray intensity wave form E (ν), then the response function for square-wave (SWR) R (ν) was calculated by the following formula,

$$R(\nu) = \frac{E(\nu)_{max} - E(\nu)_{min}}{E(\nu)_{max} + E(\nu)_{min}} \qquad (3)$$

where ν is the spatial frequency and $E(\nu)_{max}$ and $E(\nu)_{min}$ are the maximum and the minimum values of X-ray intensity waveform at each spatial frequency respectively. Moreover, the experiment on SRchart was performed by the same procedure as above.

4–2. Results of measurement and consideration

Fig. 12 shows the results of measurement in which the values of response function are given without normalization. But there is a remarkably large difference between these values of response function obtained by using KR-chart and SR-chart. As already mentioned this difference comes from the fact that the contrast characteristic of KR-chart is far better than that of SR-chart.

In the case of KR-chart, it is noticed that in the high-frequency region of more than 2.0 lines/mm the correspondence between the distance from film to deseased part and the attenuating behavior of SWR is manifested as an obvious difference in good order. This fact means that in case of detecting a minute diseased part, it is more advantageous for the diseased part exists nearer to film.

That is the diseased part nearer to the film bring about clearer images of less obscurity, and they give more reliable findings.

This fact supports the reasonableness of hitherto-used photographing technique quantitatively that we have been trying to get less obscure image by photographing close to the photographed body.

In the plot of Fig. 12, the magnification α is at most about 1.1 even at the position of D where the film is most separated from the chart, and hence in Fig. 12, the plotting against the abscissa in this case the plotting the spatial frequency was done by taking $\alpha = 1.0$ in every case, i.e., plotting the spatial fequency of chart itself.

As a special case there are some researches for the enhancement of the detecting accuracy of fine image

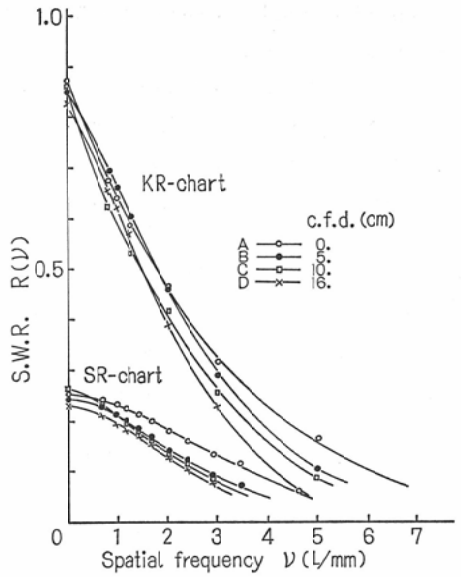

Fig. 12. The results of application measurement, where the values of square wave response are not normalized.

structures by the magnified-photographic method[3)4)5)], but in the present experiments the application of KR-chart to the close-photographic method using the X-ray absorbing bodies almost equivalent to the human body was done.

This means that a quantitative examination was performed to the most standerdized photographing system adopted nowadays.

The same experiments as above were carried out for the SR-chart.

The results of measurement are shown in Fig. 12. The SWR characteristics of the SR-chart having almost the same trend qualitatively as in the KR-chart were obtained, but the values of R (ν) are smaller than that of the KR-chart over the whole frequency range and it was observed that the cut-off frequency, i.e., resolving power of SR-chart is smaller than that of the KR-chart.

As one of the most important factor for such a result the chart contrast mentioned at the initial part of section 3.1 is conceivable.

As is evident from Fig. 8, the contrast of SR-chart is extremely smaller than that of KR-chart and the value of response function derived from the SR-chart is also smaller than that of the KR-chart.

The present experiments dealt with the measurement of spatial frequency of the photographed subjects of different contrasts which were scattered inside on X-ray absorbing body approximately equivalent to a human body and several interesting results were obtained as shown in Fig. 12. Such a trial would be a basic method to obtain the X-ray images that contain much amount of physical information and boast of high diagnostic accuracy.

5. Conclusion

Test charts of high contrast for measuring the sharpness of radiographic images were constructed by

the combination of aluminum and lead foils. The arrangement of spatial frequencies of the chart were 0(0.05), 0.85, 1.0, 1.25, 1.65, 2.0, 2.5, 3.0, 5.0, and 10.0 lines/mm and the respective frequency were composed of square wave patterns of 1.0 mm in thickness. The characteristics of these charts (KR-charts) were measured by the X-ray photographic method.

The results obtained are as follows:

In the medical diagnostic region of X-ray tube voltage (50—100 kVp) and of photographic density range (D = 0.5—2.0) it was confirmed that, as shown in Fig. 8, while the conventional test charts have their chart contrast C_E from about 0.4 to 0.7, the KR-chart shows a high value of about 0.9 over the whole diagnostic region, in other words, the KR-chart has an excellent character as a high contrast chart.

Next, the aspect of variation of response function by the change of incident angle X-ray radiation to the test chart was investigated as the incident angle characteristic.

Excepting the case of perpendicular incidence, it had been expected that the KR-chart consisting of 1.0 mm thick patterns would lower the response function to a fairly large amount as compared with the 50 μ thick evaporation-type chart (SR-chart), but actually it was confirmed from our experimental results shown in Fig. 10 that although notwithstanding the value of coefficient η showing the rate of shady part S is larger than that of SR-chart (about 20 times at the same incident angle and at the same frequency), the value of response function is better than expected.

For example, the response function characteristic of KR-chart at $\eta = 1.0$ was almost the same as that of SR-chart of $\eta = 0.1$.

This fact signifies the excellence of KR-chart to SR-chart in the structure for transmission and absorption of X-ray and also leads to the high contrast characteristic of KR-chart.

Further, we attempted, as an application of the trially made KR-chart, to simulate the test chart as a diseased part of human body, by setting it variably within a chest phantom made of synthetic resin, we obtained the response function of X-ray photograph when the distance between the chart and film (cfd) was changed to compare the response function with the sensible sharpness of diseased part. The distance cfd was taken at 0, 5, 10 and 16 cm. Based on the results of measurement shown in Fig. 12, it was found quantitatively that there is a tendency of decrease of the valued of response function gradually with increase of cfd.

For example, at frequency $\nu = 3.0$ lines/mm, it was confirmed that the amount of difference between these two response functions corresponding to the cfd equal 0 cm and 16 cm was about 0.1.

In this way we could obtain a quantitative assurance to the opinion that the hitherto-used standard X-ray photographing method in which the objective part (diseased part) is photographed by approaching it close to the film (this corresponds to making the value of cfd near to zero) is an appropriate method to obtain a good image quality.

Acknowledgement

The authors wish to express sincere thanks to Dr. M. Oguchi, Director of this Research and Development laboratory, and Dr. K. Koda, chief member of Research staff of the laboratory, for their continuous encouragement writing this Paper, and we also wish to thanks Mr. N. Iida, President of the Mitaya manufacture Co., Ltd. and Mr. T. Kamoshita, mechanical engineer of the Co., Ltd. for their cooperation in

traially make this KR-chart.

References

1) K. Rossman and G. Lubberts: Radiology, 80 (1966) 235.
2) K. Doi: Applied Physics, 35 (1966) 559.
3) K. Sayanagi: Applied Physics, 26 (1957) 134.
4) S. Sakuma, et al.: Nipp. Acta. Radiol., 28 (1969) 1506.
5) Y. Ayakawa, et al.: Nipp. Acta. Radiol., 28 (1968) 400